Anal Bioanal Chem (2013) 405:2505–2514
DOI 10.1007/s00216-012-6665-4

ORIGINAL PAPER

Binding kinetics of human cellular prion detection by DNA aptamers immobilized on a conducting polypyrrole

A. Miodek · A. Poturnayová · M. Šnejdárková · T. Hianik · H. Korri-Youssoufi

Received: 29 August 2012 / Revised: 12 December 2012 / Accepted: 13 December 2012 / Published online: 15 January 2013
© Springer-Verlag Berlin Heidelberg 2013

Abstract We developed a biosensor based on the surface plasmon resonance (SPR) method for the study of the binding kinetics and detection of human cellular prions (PrP^C) using DNA aptamers as bioreceptors. The biosensor was formed by immobilization of various biotinylated DNA aptamers on a surface of conducting polypyrrole modified by streptavidin. We demonstrated that PrP^C interaction with DNA aptamers could be followed by measuring the variation of the resonance angle. This was studied using DNA aptamers of various configurations, including conventional single-stranded aptamers that contained a rigid double-stranded supporting part and aptamer dimers containing two binding sites. The kinetic constants determined by the SPR method suggest strong interaction of PrP^C with various DNA aptamers depending on their configuration. SPR aptasensors have a high selectivity to PrP^C and were regenerable by a brief wash in 0.1 M NaOH. The best limit of detection (4 nM) has been achieved with this biosensor based on DNA aptamers with one binding site but containing a double-stranded supporting part.

Keywords Prions · Aptamers · Kinetics · SPR · Polypyrrole

Electronic supplementary material The online version of this article (doi:10.1007/s00216-012-6665-4) contains supplementary material, which is available to authorized users.

A. Miodek · H. Korri-Youssoufi (✉)
CNRS UMR-8182, Institut de Chimie Moléculaire et des Matériaux d'Orsay, Equipe de Chimie Bioorganique et Bioinorganique, Univ Paris-Sud,
Bâtiment 420,
91405 Orsay, France
e-mail: hafsa.korri-youssoufi@u-psud.fr

A. Poturnayová · M. Šnejdárková
Institute of Animal Biochemistry and Genetics, Slovak Academy of Sciences, 900 28 Ivanka pri Dunaji, Slovakia

T. Hianik
Faculty of Mathematics, Physics and Informatics, Comenius University, Mlynska dolina F1,
84248 Bratislava, Slovakia

Introduction

The diagnosis and treatment of neurogenerative diseases, such as Alzheimer's or Creutzfeldt–Jakob, are priorities under consideration for health institutions. It is assumed that these diseases are caused by transformation of cellular prions (PrP^C) into their infectious isoform PrP^{Sc} [1, 2]. PrP^{Sc} differs from PrP^C in its insolubility, high content of β sheets, partial resistance to protease digestion, and tendency to form large aggregates [3]. Therefore, the development of a rapid and sensitive method for the detection of PrP^{Sc} is crucial for early diagnostics of these diseases. Especially useful would be a point-of-care assay that can be used even by physicians outside of specialized clinical laboratories [4]. So far, mostly the immunodiagnostic procedure [5] and postmortem histopathological identification of brain tissues were applied [6–13]. However, in contrast with cerebrospinal fluid, the concentration of PrP^{Sc} in the blood is down to the pM level, which makes the measurement difficult to achieve. Therefore, a special analytical approach is required. Biosensor technology can be a possible option. According to the WoS database, the first attempt to construct such a biosensor for the detection of prions was made by Cuccioloni et al. [14]. They developed the resonant mirror biosensor using plasminogen for the detection of recombinant (PrP^C (25–242)) and natural cellular prions. The detection was based on the affinity of PrP^C to a plasminogen—a serum protease which is a natural component in the blood [15]. The binding of recombinant PrP^C to plasminogen

was characterized by higher kinetic association constant in comparison with that for natural cellular prions. The possible reason is due to the presence of carbohydrate moieties in natural prions that sterically hinder intermolecular protein-protein interactions. Recently, detection of recombinant PrP^C by electrochemical quartz crystal microbalance (EQCM) biosensor was reported [16]. The detection was based on the sensitivity of quartz crystal transducer to a mass loading. The monoclonal antibodies or specific DNA aptamers were immobilized on the multiwalled carbon nanotubes. PrP^C can be detected with high sensitivity and specificity down to 20 pM for antibodies and 50 pM for DNA aptamers. Surface plasmon resonance (SPR) method has been used for label-free detection of the affinity interactions (see [17, 18] and reference herein) including the kinetic of both association and dissociation processes. This method has been used in immunosensing assay for detection of bovine prion protein [19] using specific single-chain antibody (scFv-Z186-SPB) immobilized on streptavidin layer. However, the equilibrium dissociation constant (K_D) was relatively low (0.4 μM). Substantial progress in application of SPR in detection of prions such as PrP^C and PrP^{Sc} was reported recently by Wan et al. [20], within sandwich assay. The monoclonal antibodies were immobilized on the sensor surface and after the complex formation of prion proteins, the signal was amplified by addition of polyclonal anti-prion antibodies. This approach allowed detection of PrP^C with a limit of detection (LOD) of 1.4 nM. Despite high sensitivity of this assay, the amplification step by another antibody is needed. Measurement in real time with SPR method requires both suitable platform for the immobilization and sensitive bioreceptor for molecular recognition. We demonstrated previously that modified conducting polypyrroles bearing biotin streptavidin system are a good platform for antibody immobilization and for the study of antigen–antibody interaction by SPR method [21]. Aptamers as bioreceptors were successfully used for detection of human IgE [22], human thrombin [23], and retinol binding protein [24] by SPR measurements. High-affinity DNA aptamers to PrP^C has been developed previously by Takemura et al. [25]. In this work, we developed sensitive biosensor based on conducting polypyrroles modified by streptavidin for immobilization of PrP^C-sensitive DNA aptamers. We demonstrated that the structure of the spacer of DNA aptamers (single or double strand) served for aptamer immobilization significantly affects the sensitivity of PrP^C detection. The aptamer dimers containing two binding sites were also applied. The sensitivity of PrP^C detection and binding kinetics were determined by SPR method and compared for various aptamers.

Materials and methods

Chemicals

The recombinant human PrP^C protein (Human PrP^C (103–231)) molecular weight 15.1 kDa and the PrP^C (23–124) molecular weight 11 kDa used as nonspecific control were purified in INRA Jouy-en-Josas, France, by Dr. Human Rezaei and Jasmina Vidic. BSA was obtained from Sigma-Aldrich (USA). The DNA aptamers specific for PrP^C were designed according to Takemura et al. [25] and purchased from Thermo Fisher Scientific (Ulm, Germany) together with oligonucleotide dA_{15}. DNA aptamers contained dT_{15} spacer (5′-CGGTGG GGCAAT TTC TCCTACTGT dT_{15}-3′-biotin) and bearing biotin in 3′-position, the other aptamers constituted with dA_{15} as spacer 5′-dA_{15}-AGTCATCCTTTCAATG GCTGGCGG-3′.

The formation of aptamer dimers (Biopri-Compri) and conventional aptamers Biopri containing double stranded supporting part ($dsA_{15}T_{15}$) have been obtained by mixing equal volumes (0.5 ml) of equimolar concentrations (2 μM) of respective single stranded oligonucleotides (see Table 1), incubating them at 35 °C during 1 h with subsequent cooling to room temperature (20 °C).

The biotinylated DNA aptamers were immobilized on a polypyrrole bearing streptavidin (see Section 2.2. for the method of sensor preparation). For this purpose, the following reagents were used. Pyrrole (py) was purchased from Sigma-Aldrich, and distilled under argon before use. Biotin hydrazide and streptavidin were purchased from Sigma-Aldrich. The 3-(*N*-hydroxyphthalimidyl ester) py was synthesized according to a method described elsewhere [21, 26]. Other chemicals used were of p.a. grade. Phosphate-buffered saline (PBS) composed of 10 mM Na_2HPO_4, 1.8 mM KH_2PO_4, 2.7 mM KCl, and 137 mM NaCl, pH=7.4, has been used as a binding buffer. The Millipore water (Millipore, El Paso, USA) was used for preparation of buffers.

Preparation of aptamers-based biosensor on conducting copolypyrrole

The copolymer film, poly[pyrrole, 3-*N*-hydroxyphthalimido pyrrole] (copoly(py-pyNHP) was grown on a gold surface (of prism or quartz crystal) in an electrochemical cell containing 50 μl of a 10-mM solution of py and 3-*N*-hydroxyphthalimido pyrrole (pyNHP) monomers and 0.5 M $LiClO_4$ in acetonitrile. We used the ratio of the py/pyNHP 8:2 that has been previously reported as optimal for detecting antigen-antibody interactions and avoiding a steric effect [21]. Electropolymerization was performed by cycling the potential from −0.4 to 1.2 V vs. Ag/AgCl reference electrode and the reaction was stopped when the current reached

Table 1 The structure of DNA aptamers

Name	Structure of DNA aptamer
Biopri	5′-CGG TGG GGC AAT TTC TCC TAC TGT dT_{15}-3′-biotin
Biopri-Comp	5′-CGG TGG GGC AAT TTC TCC TAC TGT ds $A_{15}T_{15}$–3′-biotin
Biopri-Compri	5′-CGG TGG GGC AAT TTC TCC TAC TGT5′-CGG TGG GGC AAT TTC TCC TAC TGT ds $A_{15}T_{15}$–3′-biotin

40 μA. The modified surface was rinsed with acetonitrile and three times with PBS in order to remove any trace of monomers. The kinetic of polymerization reaction demonstrating the variation of the angle vs. time was recorded during the polymerization reaction. The sensogram presenting the variation of reflectivity vs. angle was recorded in PBS before and after the polymerization reaction.

The aptasensor was constructed as follows. Biotin was covalently bounded on copoly(py-pyNHP) at the surface of electrode in SPR cell by adding 50 μl of a 2-mgml^{-1} solution of biotin hydrazide in PBS and incubation during 15 min at room temperature. The resulting biotinylated py film was washed five times with the same buffer followed by the addition of 50 μl of 100 μgml^{-1} streptavidin solution during 15 min. Afterwards, 50 μl of 2 μM biotinylated aptamer in buffer was added to this surface and incubated for 30 min. Then the electrode was carefully washed five times with PBS. The PrP^C was deposited on a sensor surface. After addition of PrP^C in a respective concentration and reaching steady-state value of the angle, the surface was washed by flow of PBS. The regeneration of the sensor was performed by washing its surface with 0.5 M NaOH during 3 s and then with PBS. Each step in the aptasensor preparation was directly monitored by SPR method. Scheme 1 shows the main steps of the preparation of sensing layer.

For QCM measurement, the polymerization was performed with the same procedure on the quartz crystal with sputtered gold electrodes (area, 0.2 cm^2). Only one side of the crystal was used for preparing the sensing layer. The same steps as described above were used for preparation of aptasensor in the flow cell with flow rate 50 μlmin^{-1}.

SPR and QCM measurements

An AUTOLAB ESPRIT double-channel instrument (Eco Chemie, Utrecht, The Netherlands) was used to perform optical detection of the SPR angle and electrochemical measurements with an incorporated auto-sampler. A polarized laser light (λ=670 nm) was directed to the bottom side of the sensor via a hemispheric lens placed on a prism (BK7 with a refractive index of 1.52) and the reflected light was detected using a photodiode. The standard electrochemical cell allowed measurements using a three-electrode system containing a fixed contact point to the gold layer of the sensor disk that served as working electrode, a replaceable Ag/AgCl reference electrode and a fixed platinum counter-electrode. The active electrode surface was 0.06 cm^2. Electrochemical polymerization was performed using an AUTOLAB PGSTAT 12 monitored by GPES by means of the above mentioned electrochemical cell (see Lê et al. [21] for more details).

QCM measurements were performed using a home-made apparatus based on SN74LS320 crystal-controlled oscilator (Texas Instruments, USA) and constructed according to Skladal and Horacek [27]. The changes in oscillation frequency were measured by means of UZ 2400 frequency meter (Grundig, Germany) connected to IBM PC Pentium through a RS232 interface. The frequency was measured with 1 Hz accuracy. For the preparation of the affinity biosensor we used AT-cut quartz with a fundamental frequency of 8 MHz (CH Instrumnets, USA), covered on both side by polished gold electrodes (working area, 0.2 cm^2). The crystal was cleaned in ultrasound bath type sonicator (DT-31, Bandelin Electronic, Germany) during 30 min in 0,1 % sodium dodecyl sulphate, then 15 min in Millipore water, 5 min in acetone, 5 min in ethanol, and 5 min in methanol. After cleaning, the crystal was dried in a stream of nitrogen and then immersed into the EQCM cell (CH Instrument) in which the copoly(py-pyNHP) layer was formed according to procedure described in Section 2.2. Then the crystal was mounted in the flow-through cell (the cell was a gift from prof. M. Thomson, University of Toronto and is described in Ref. [28]). The buffer and analytes were introduced into cell by means of a Genie Plus syringe pump (Kent Scientific, USA).

Results and discussion

The SPR method was applied to study the biosensors formation as well as kinetics of binding and detection of PrP^C with DNA aptamers of various configurations. The aptamer's selectivity was also examined. The biotinylated DNA aptamers were immobilized on a sensor surface composed of conducting co-polymer(py-pyNHP) with immobilized biotin/streptavidin layer.

Copolymer film formation

The copoly(py-pyNHP) film was formed at a gold support by cycling the potential from −0.4 to 1.2 V (vs. Ag/AgCl reference electrode). Figure 1 shows the increase of current

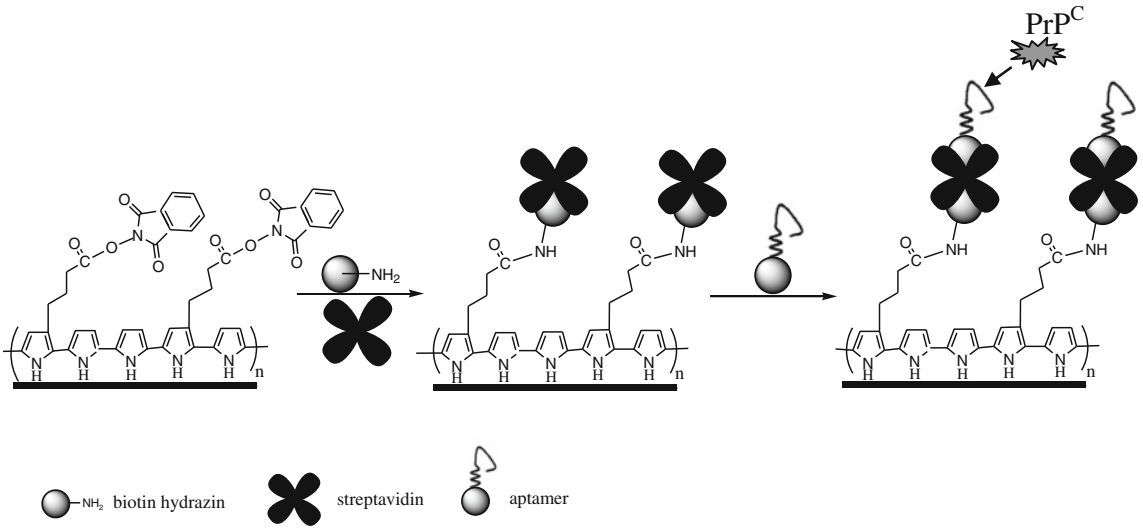

Scheme 1 Schematic representation and synthetic procedure for the construction of the aptasensor: (**a**) electropolymerization of copoly(py-pyNHP) film at the electrode surface, (**b**) covalent grafting of biotin on copoly(py-pyNHP) layer and immobilization of streptavidin via biotin, and (**c**) anchoring of biotinylated aptamer on polypyrrole–biotin–streptavidin double layer

of redox signal of polypyrrole as well as the increase of the angle during the polymerization reaction. The increase of peak current after each scan (Fig. 1a) demonstrates that the conductive film is formed on the gold surface. The polymerization reaction was monitored simultaneously also by SPR method (Fig. 1b, c). The kinetic of the variation of the angle vs. time during the polymerization reaction demonstrates an increase of the refractive angle after each CV scan. The variation of the angle is related to the changes of refractive index of the gold layer due to the deposition of polypyrrole on the gold surface of the prism (Fig. 1b). The kinetics of reaction shows a continuous increase of the angle after each cycle demonstrating that the polymerization of the two monomers leads to homogenous copolymer film. The plasmon resonance curve (Fig. 1c) obtained at open circuit potential before (curve a) and after (curve b) polymerization in the same PBS shows an increase of the resonance angle from 69.4° to 70.2°, respectively. The fitting of the experimental curve to theoretical one allows calculating the thickness of the polypyrrole layer determined to be 8 nm. The fitting was performed by winspall program using the same parameters as reported previously [21].

Formation of aptamers sensing layer

Immobilisation of DNA aptamers bearing biotin group was performed similarly to the method reported recently for antibodies [21]. The analysis of all steps necessary for immobilization of DNA aptamers on a poly(py-pyNHP) surface was performed by both SPR and QCM methods. Both methods allow determining the binding kinetic. In SPR method, the change in the angle is related to the amount of molecules immobilized on the film. The changes in angle, $\Delta\Theta$, of reflected light following various modification of the py-pyNHP surface are shown in Fig. 2a. Addition of 2 $mg ml^{-1}$ of biotin leads to a change in the SPR angle by 61 m° indicating a covalent attachment of biotin hydrazide to the pyNHP unit and the formation of a stable amide link in the poly(py-py-Bio) surface. When 100 $\mu g ml^{-1}$ of streptavidin was added, the SPR angle increases considerably (246.9 m°), which is in good agreement with larger size of streptavidin and thus with thicker layer formed in comparison with that of biotin. Thus, due to high affinity of streptavidin to biotin a stable streptavidin film was formed poly(py-py-Bio-Strep). The injection of 2 μM of biotinylated DNA aptamers increases the SPR angle by 23 m° confirming their immobilization via the biotin–streptavidin interactions.

Similar behavior was observed during the formation of sensing layer using QCM technique. This method allows evaluation of the change in mass by measuring the frequency after such reaction on the surface l of polypyrrole layer. The decrease in frequency is connected with increase of the mass, Δm, of the quartz crystal surface in accordance with Sauerbrey equation [29]:

$$\Delta f = -2.26 \times 10^{-6} f_0^2 (\Delta m / A) \quad (1)$$

Where A is the area of the working electrode (0.2 cm^2) and f_0 is the fundamental frequency of the crystal (in our case f_0=7.98 MHz)

Decrease in frequency was measured after covalent attachment of biotin and interaction of streptavidin followed by aptamer immobilization. Figure 2b shows the kinetics of the resonant frequency changes following various modifications

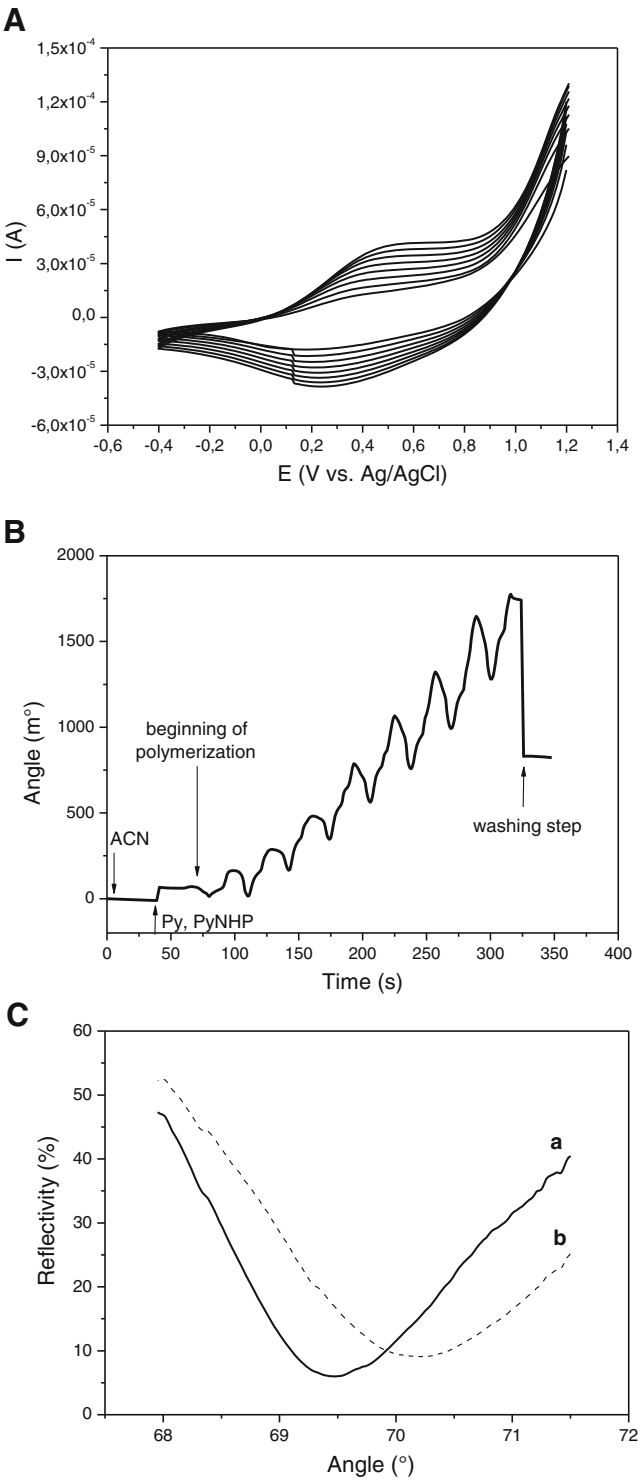

Fig. 1 (**A**) Cyclic voltammograms obtained during the polymerization of copolymers poly(py-py-NHP) in 0.5 M $LiClO_4$ dissolved in acetonitrile (*ACN*) at scan rate 100 mV s^{-1}. Voltage is vs. Ag/AgCl reference electrode. (**B**) SPR kinetic curve obtained during the polymerization reaction. (**C**) Sensogram obtained in 10 mM PBS (a) before polymerization reaction and (b) after the formation of the copolypyrrole film on the gold surface

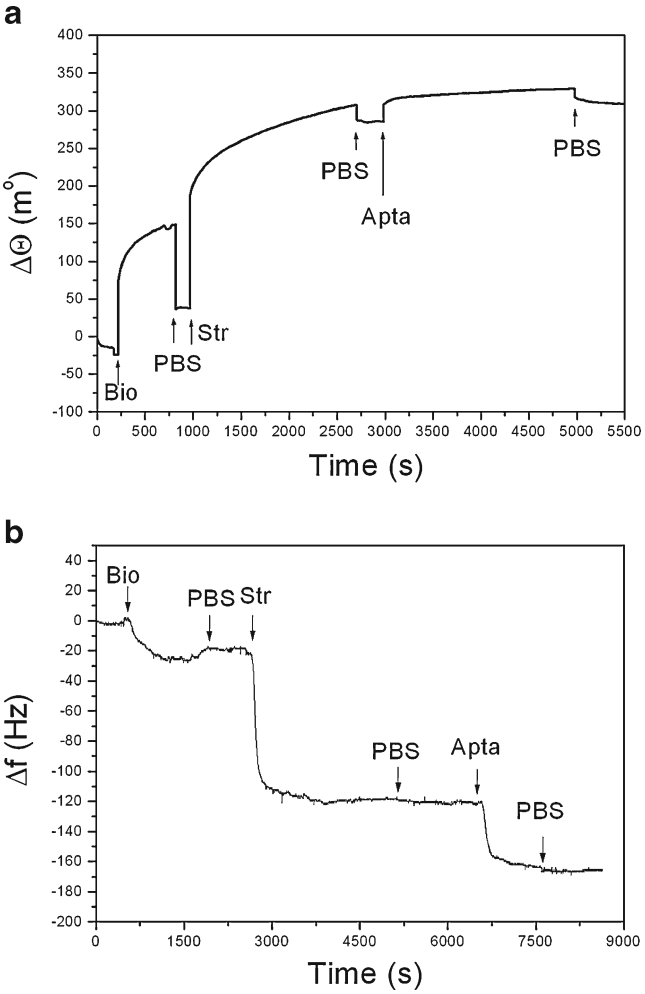

Fig. 2 (**a**) SPR kinetic curve of different steps of biosensor construction: immobilization of biotin (*Bio*; 2 mg ml^{-1}), streptavidin (*Str*; 100 μg ml^{-1}), and biotinylated DNA aptamer (*Apta*; 2 μM) followed by washing of the sensor by PBS. (**b**) Changes in resonant frequency as a function of time during biosensor formation with the same procedure as for SPR

of poly(py-pyNHP) layer deposited on quartz crystal transducer. It can be seen, that addition of 2 mg ml^{-1} of biotin resulted in decrease of the resonant frequency by approximately 30 Hz. The final frequency changes after washing the surface by PBS were 20 Hz. This result confirms the formation of stable biotin layer strongly attached to poly(py-py-Biot) surface. Flow of streptavidin in a concentration 100 μg ml^{-1} caused sharp decrease of resonant frequency which demonstrates a strong affinity of streptavidin to biotin. The changes of resonant frequency after washing the surface with PBS were 80 Hz which is much larger in comparison to that caused by biotin and agree with higher molecular weight of streptavidin. Earlier works indicated that streptavidin forms rather rigid layers with minor contribution to the surface viscosity [28]. Thus, the change in frequency can be attributed mostly to the mass effect. Therefore Eq. (1) can be used for estimation of the mass

changes and the surface coverage. According to this equation, the changes in resonant frequency 80 Hz correspond to the mass changes of 111 ng. Taking into account that the molecular weight of streptavidin is 60 kDa and the surface of electrode is 0.2 cm^2, the average coverage of streptavidin is 9.25 $pmol\,cm^{-2}$.

Addition of conventional single stranded aptamer, Biopri, resulted on further decrease of the resonant frequency by 42 Hz. This corresponds to aptamers surface concentration of 23 $pmol\,cm^{-2}$. The aptamer immobilized on the surface is about 2.5 times higher in comparison with surface concentration of streptavidin. However, brush-like surface of the sensor with immobilized aptamers interacts more extensively with the surrounding buffer. This interaction typically results in additional frequency decrease due to viscosity effect [30]. Therefore, the aptamers surface density can be up to 50 % lower in comparison to that calculated from frequency changes [31]. Thus, around 1 to 2 binding sites of streptavidin molecule participate on aptamers binding. Taking into account that streptavidin has four binding sites for biotin and presumably two sites are involved in the interaction with copolymers surface, the obtained estimation is reasonable. Binding of Biopri-Comp aptamers (i.e., Biopri aptamers containing double stranded supporting part) show similar surface concentration like Biopri, 20 $pmol\,cm^2$. However when Biopri-Compri aptamers with two recognition sites were immobilized on streptavidin layer, the average coverage decreases to 14 $pmol\,cm^{-2}$. This is due to a large surface area of the aptamers containing two binding sites. The results obtained by QCM method are summarized in Table 2.

Detection of PrP^C using SPR method

The kinetic of interaction of the PrP^C with biosensors formed by various DNA aptamers was studied by measurement of SPR angle changes after addition of PrP^C in different concentrations. Figure 3 shows the changes of angle for biosensors formed with copolypyrrole modified with Biopri, Biopri-Comp and Biopri-Compri, any variation of the angle was observed after prion addition when aptamers were not immobilized on the surface (see Fig. S1 in the Electronic

Table 2 Changes in resonant frequency, Δf, mass, Δm, calculated using Sauerbrey Eq. (1) and surface concentration of aptamers of various configurations immobilized at streptavidin layer of the sensor

Aptamer	Δf (Hz)	Δm (ng)	Surface concentration ($pmol\,cm^{-2}$)
Biopri	42	58	23
Biopri-Comp	50	69	20
Biopri-Compri	54	75	14

The values of Δf were derived from kinetic curves like that presented on Fig. 2b. The SD calculated from three measurements does not surpass 10 %

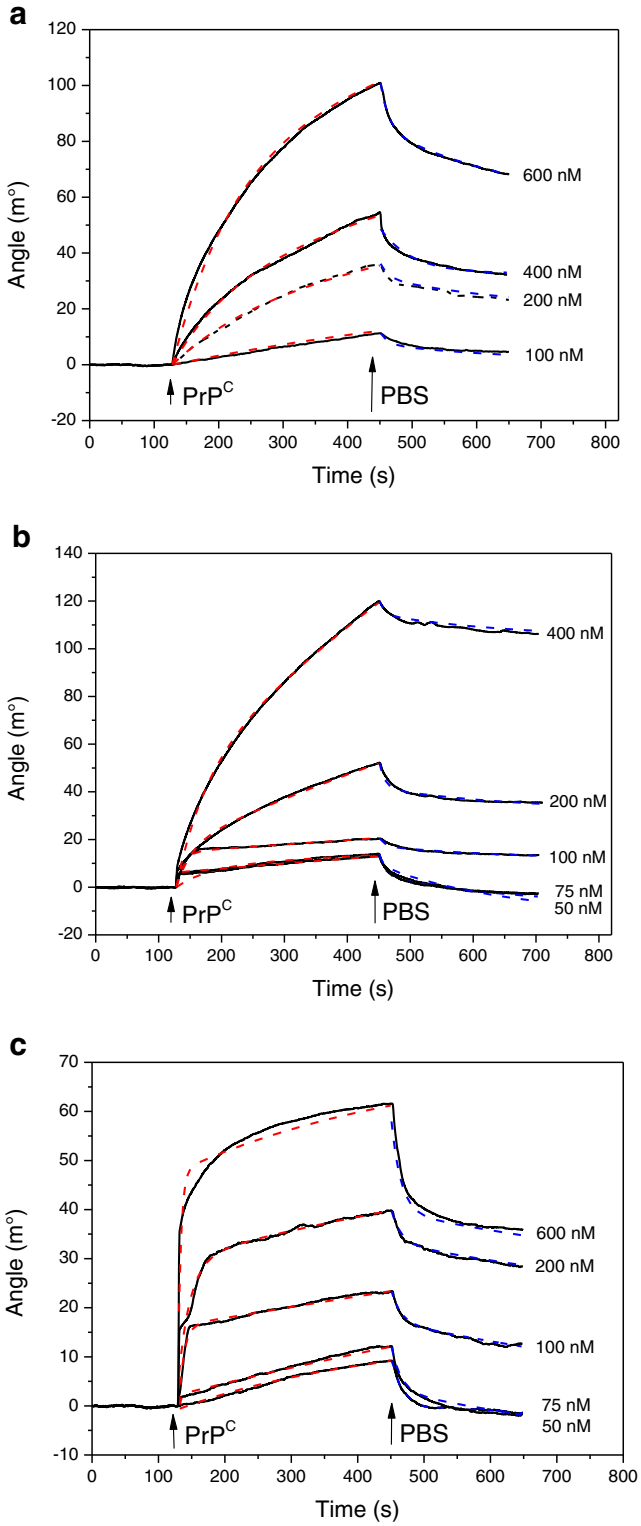

Fig. 3 SPR kinetic curve as a function of PrP^C concentrations for biosensors with immobilized aptamers of various configurations. *Full lines*, experimental curve; *dashed line*, fitting curve (**a**) Biopri, (**b**) Biopri-Comp, and (**c**) Biopri-Compri

supplementary material). The kinetic of association was recorded and followed by dissociation step. It can be seen that addition of relatively small concentration of PrP^C between 50 and 100 nM results in substantial increase of SPR angle by more than 40°m. This value was taken as a difference between initial angle, prior addition of the protein and after washing the sensor surface with PBS buffer solution (the washing of the surface by PBS resulted in removing of nonspecifically adsorbed PrP^C molecules). The surface regeneration was performed by application of the flow of 0.1 M NaOH with subsequent washing by PBS and resulted in almost recovery of the initial SPR angle. After regeneration, the sensor was again sensitive to PrP^C as it is seen from the changes of the angle after subsequent addition of PrP^C. From SPR binding curve we can observe that depending on the aptamer configuration the variation of the angle vs. the concentration is different.

In order to analyze quantitatively the kinetics of PrP^C binding to DNA aptamers of various structures, the rate constant of association (k_a) and dissociation (k_d) can be calculated from the SPR binding curves showed in Fig. 3.

The binding reaction of PrP^C with aptamer immobilized at the surface can be described as follows:

$$[Aptamer] + \left[\mathrm{Pr}\,P^C\right] \underset{k_d}{\overset{k_a}{\rightleftharpoons}} \left[Aptamer/\mathrm{Pr}\,P^C\right] \tag{2}$$

The formation of the complex [aptamer/PrP^C] is measured in real time with the SPR binding curve and the following equation developed for protein binding reaction could be applied [32]

$$\frac{\mathrm{dR}}{\mathrm{dt}} = k_a C R_{\max} - (k_a C + k_d) R_t \tag{3}$$

The kinetic rate parameters can be determined by means of integrated rate analysis method using following equations:

$$R_t = \frac{k_a C R_{\max}\left[1 - e^{-(k_a C + k_d)t}\right]}{k_a C + k_d} + R_0 \tag{4}$$

$$R_t = E\left(1 - e^{-k_s t}\right) + R_0 \tag{5}$$

$$E = k_a C R_{\max}/(k_a C + k_d) \qquad k_s = k_a C + k_d \tag{6}$$

where R is the SPR signal, C is the concentration of the protein PrP^C in solution, R_{max} is the maximal change in response to a certain PrP^C concentration, R_t is the response obtained at time t and R_0 is the response at t=0. These parameters could be calculated by nonlinear fitting of binding curves with various concentrations of PrP^C using Eq. (4). Equation (5) describing the association phase of a macromolecular complex for one to one interaction. The kinetic information is obtained from parameter k_s. A plot of k_s values vs. concentration is used to obtain the values of k_a and k_d from Eq. (6). The dependence of k_s on concentration PrP^C should be a straight line. The intercept of the line with ordinate gives the k_d value, while the k_a is equal to the line slope. The k_d value could be calculated also by fitting the dissociation curve.

However, considering that biosensor constructed with DNA aptamers (Biopri-Compri) has two sites for interaction with PrP^C, the binding curves were fitted also with another model, i.e., two biphasic interaction. This model allows to analyze binding of PrP^C to the two sites of aptamer with different affinity. The biphasic model based on two equilibrium constants is described by Eq. (7)

$$R_t = \left[E_1\left(1 - e^{-k_s(1)t}\right) + E_2\left(1 - e^{-k_s(2)t}\right)\right] + R_0 \tag{7}$$

Where $k_s(1) = k_{a(1)}C + k_{d(1)}$ and $k_s(2) = k_{a(2)}C + k_{d(2)}$ are related to the kinetic of the rate constant of association and dissociation of the PrP^C to the recognitions sites of aptamers.

The binding curve obtained with biosensor based on aptamer dimers does not fit the theoretical model of monophasic interaction Eq. (4). However all binding curves obtained by biosensors composed of the three types of aptamers are fitted very well with the biphasic model (Eq. (7)) (see Fig. 3). This demonstrates that affinity of PrP^C to the aptamer with one site or two site of interaction are practically the same.

The values of k_a and k_d were calculated from the fitting curves based on Eq. (5) and (6). However, as it can be seen from the Fig. 3, after relatively sharp increase of the SPR angle, more slow increase of this value took place. It is well visible especially at low PrP^C concentrations. The linear part of the kinetic curves suggests the dominant effect of the mass transport. Therefore, in determination of the kinetic constants we analyzed the kinetic curves in the time interval below 450 s where the kinetically controlled association of PrP^C to the aptamers is prevailing. The results of calculations are presented in Table 3. The k_d value was compared with those obtained by fitting the dissociation phase and same value were obtained. The equilibrium association and dissociation constants (K_A and K_D, respectively) could be determined from the k_a and k_d values: $K_A = k_a/k_d$ and $K_D = 1/K_A$. Using the above mentioned procedure the value of association and dissociation constant for biosensor based on conventional single stranded aptamers (Biopri) are $k_a = (3.3 \pm 0.2) \times 10^4 s^{-1} M^{-1}$ and $k_d = (2.0 \pm 0.3) \times 10^{-3} s^{-1}$. The rate of association constant increases for the biosensor constructed with (Biopri-Comp), i.e., containing double-stranded supporting part (see Scheme 2) $k_a = (4.5 \pm 0.5) \times 10^4 s^{-1} M^{-1}$ and remains almost unchanged for biosensor based on aptamer dimers (Biopri-Compri) $k_a = (2.8 \pm 0.2) \times 10^4 s^{-1} M^{-1}$. The equilibrium

Table 3 Kinetic rate constants of association (k_a), dissociation (k_d), equilibrium constant of dissociation (K_D), limit of detection (LOD), correlation coefficient (R), and dynamic range of biosensors based on DNA aptamers of various configurations

Aptamer	k_a ($M^{-1}s^{-1}$)	k_d (s^{-1})	K_D (nM)	LOD (nM)	Dynamic range (nM)
Biopri	$(3.3\pm0.2)\times10^4$	$(2.0\pm0.3)\times10^{-3}$	60.6±9.8	6	100–800
Biopri-Comp	$(4.5\pm0.5)\times10^4$	$(1.0\pm0.1)\times10^{-3}$	22.2±3.3	4	50–600
Biopri-Compri	$(2.8\pm0.2)\times10^4$	$(3.0\pm0.8)\times10^{-3}$	107.1±29.6	15	50–1,000

dissociation constant, K_D, is measured for PrP^C affinity to the aptamer binding site. This value did not differ significantly for Biopri and Biopri-Compri-based biosensors, but substantially lower value was obtained for Biopri-Comp-based aptasensor. The increase of association constant (or decrease of equilibrium dissociation constant, K_D for biosensor based on Biopri-Comp is related to the high surface organization due to the rigid double strand spacer. However when the aptamers dimers are immobilized on the surface of biosensor, the kinetic of interaction was not promoted. This can be due to sterical hindrance of closely located binding sites. Similar effect has been obtained also for thrombin/binding aptamers using both acoustic [33] and AFM methods [34].

The obtained kinetics constants are comparable with biosensor based on resonant mirror detection of PrP^C and plasminogen as bioreceptor [14] and higher than the value demonstrated for monoclonal antibody scFv-Z186-SPB [19] determined with SPR measurement (see Table 3). The kinetic constants are lower compared with bioreceptor constituted with (cytosine-5)-DNA methyltransferase SsoII to double stranded DNA contained specific binding site for the protein [35].

Analysis of the sensitivity

The plot of the changes in angle, $\Delta\Theta$, as a function of PrP^C concentration is presented in Fig. 4. It can be seen that the angle shifts is proportional to the amount of captured protein PrP^C. The SPR angles variation show a non linear dependence on the bulk concentration of protein. This behavior is expected from immunosensor and could be expressed by theoretical Eq. (8) for SPR binding angle at equilibrium:

$$\theta = \theta_{max}\frac{K_A[PrP^C]}{(K_A[PrP^C]+1)} \quad (8)$$

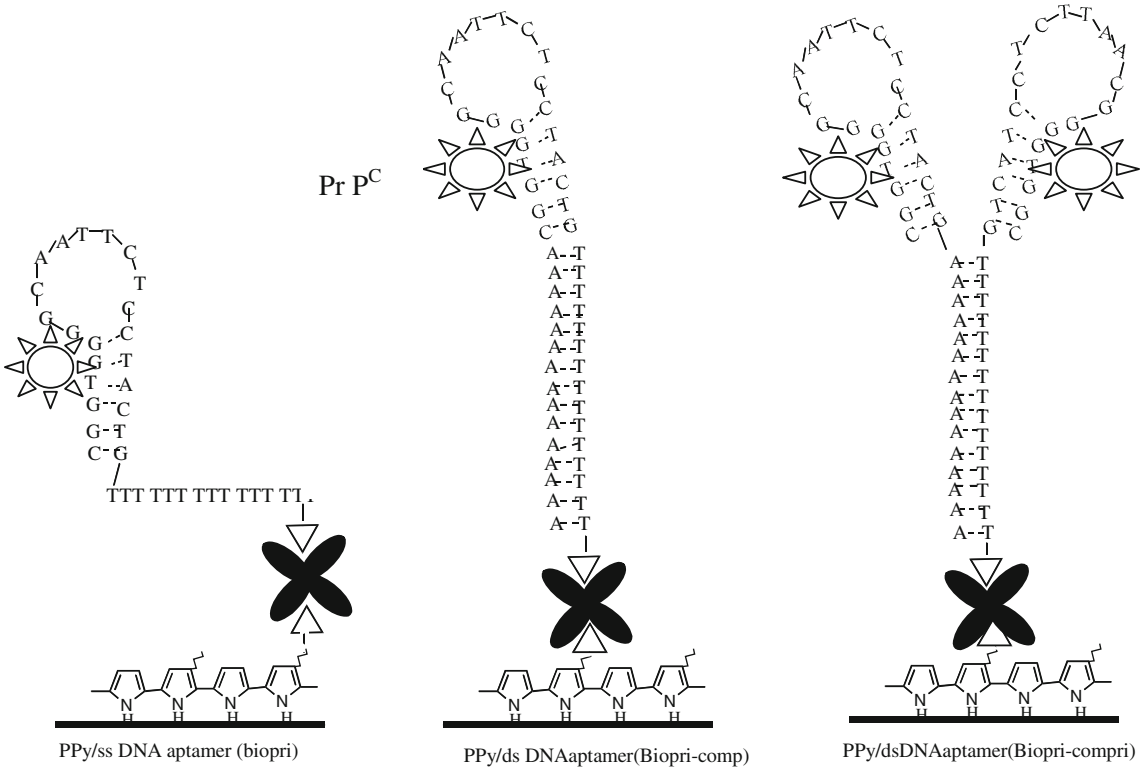

Scheme 2 Structure of the biosensors obtained for aptamers of various configurations

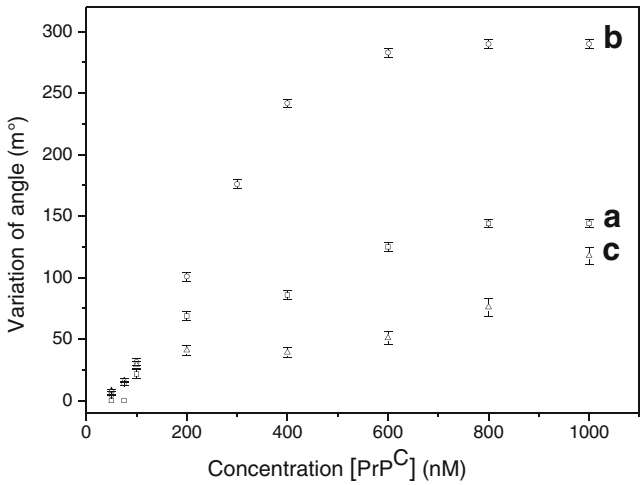

Fig. 4 SPR calibration curves obtained for biosensors based on aptamers of various configurations. (**a**) Biopri, (**b**) Biopri-Comp, and (**c**) Biopri-Compri

Where K_A is the equilibrium binding constant ($K_A=k_a/k_d$) and [PrP^C] is the concentration of prion protein. The maximal changes of SPR angle allow to calculate approximately the amount of PrP^C immobilized on the biosensors at saturation. The variation in the angle is related to the immobilized protein. The surface concentration of 100 ngcm^{-2} corresponds to 120°m [18]. Thus, the concentration of prion protein immobilized on the surface of biosensors depends on the aptamer configuration and varied from 8.6 pmolcm^{-2} for biosensor formed with Biopri to 13.8 pmolcm^{-2} for biosensor formed with aptamers Biopri-Comp and decrease to 6.6 pmolcm^{-2} for the biosensor formed with Biopri-Compri. This agrees with the observed tendency in aptamer immobilization (see Table 2).

The sensitivity of the biosensor was evaluated through the linear relationship obtained for plot of the changes in SPR angle as a function of the concentration of PrP^C at low concentration. The variation of angle vs. concentration of PrP^C is described by straight line for all biosensors at low concentration less than 200 nM. From these curves, LOD is determined using common criteria of significant analyte detection at the level corresponding to signal to noise ratio (S/N=3, the noises of SPR apparatus were approximately 1°m). The results of calculation of above-mentioned parameters are presented in Table 3 and demonstrate that the LOD of the biosensors formed by the Biopri, Biopri-Comp, and Biopri-Compri. aptamers are 6, 4, and 15 nM, respectively. The lower detection limit is obtained for biosensors based on Biopri-Comp aptamers with one binding site and containing double-stranded supporting part. The comparison of the LOD values for aptasensors obtained in this work with those based on SPR measurements using other bioreceptors a recognition element show that the present biosensors has sensitivity compared with biosensor with plasminogen as bioreceptor whith (LOD=2.4 nM) [14]. At the same time the SPR biosensor for detection PrP^C using monoclonal antibodies and amplification of the signal by polyclonal antibodies [20] has higher sensitivity (LOD=0.57 nM). The DNA aptamers are a substantial advantage over antibodies due to their direct analysis without amplification step and has high stability and lower price in comparison to monoclonal antibodies.

The analysis of aptasensor selectivity was studied in presence of BSA and N-terminal part of PrP^C (23–124) protein and compared with the result obtained with PrP^C (103–231) (Fig. 5). We can see from Fig. 5a that the biosensor show very small variation of angle in presence of nonspecific prion protein (3°m), however, the variation is very large with the specific prion protein PrP^C (103–231) with the biosensors composed of aptamers with various structures. Figure 5b shows the variation of the angle after such interaction with increasing concentration of PrP^C (103–231), PrP^C (23–124), and BSA. Small variation of

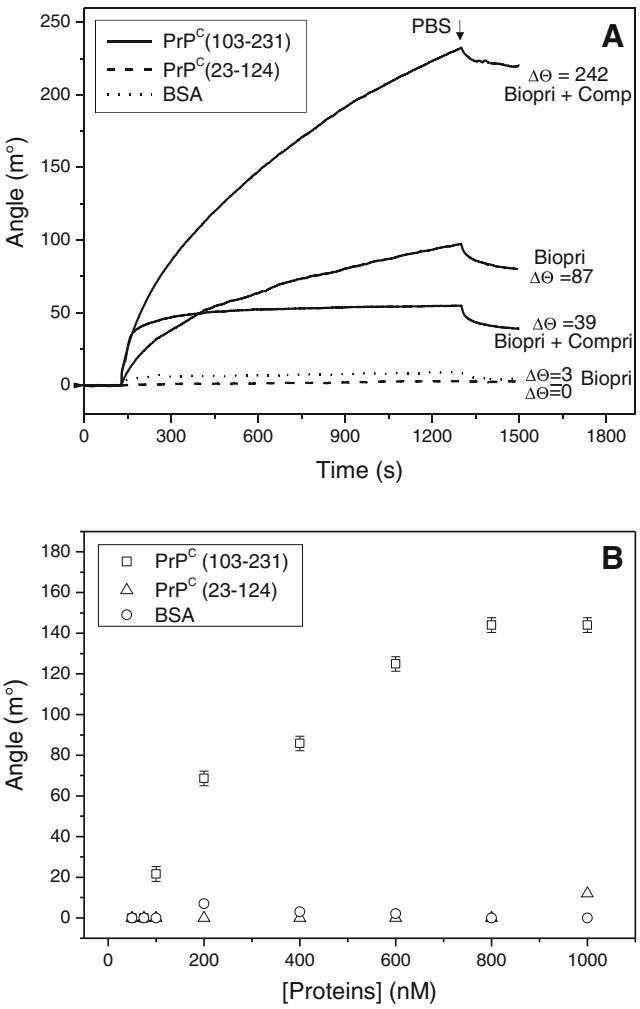

Fig. 5 (**A**) Comparison of SPR kinetic curves obtained with the biosensors based on DNA aptamers of various configurations following addition of 400 nM PrP^C (103–231), 400 nM PrP^C (23–124), and 400 nM BSA, (**B**) calibration curves obtained with Biopri aptasensor for various prions and BSA

the SPR angle was obtained for high concentration of PrP^C (23–124) and BSA compared with those of PrP^C (103–231). These results demonstrate the high selectivity of this sensor to the structural part of the human protein PrP^C (103–231) and not to the N-terminal part (PrP^C (23–124)) and demonstrate that the surface layer of polypyrrole did not affect the selectivity of the biosensors. The same results were obtained with EQCM aptasensor that can detect PrP^C in a buffer containing 3 mM BSA and suggest that BSA interaction with aptamers are negligible [16].

Conclusions

In this work, we reported the study of the kinetics of binding PrP^C to DNA aptamers of various configurations immobilized on the surface of conducting polypyrrole using SPR. The reported approach can serve as a basis for the construction of sensitive biosensor for the detection of prion proteins. We demonstrate, that these SPR aptasensors allow detection of PrP^C protein with high sensitivity and selectivity. Biosensors based on DNA aptamers containing rigid supporting part formed by double stranded DNA allow detection of PrP^C with higher sensitivity in comparison with conventional single-stranded aptamers. However, the aptamer dimers containing two recognition sites for PrP^C are less sensitive and are characterized by lower association rate constant, which is related to the steric effect. SPR aptasensors constructed by immobilization of DNA aptamers on polypyrrole layer shows sensitivity compared with other bioreceptors such as antibodies and has the advantage of regeneration using simple method of washing the sensor surface with 0.1 M NaOH. We should note that the same approach could be developed for detection of pathological forms of prion (PrP^{Sc}) using adequate aptamer which will be able to interact with PrP^{Sc} protein.

Acknowledgements This work was supported by the Slovak Research and Development Agency (contracts No. APVV-0410-10, SK-FR-0025-09), by France Government, by Slovak Academy of Sciences under the project mnt-era.net (proposal No. 2009-50) and VEGA (project No. 1/0785/12). We are grateful to Dr. Human Rezaei and Dr. Jasmina Vidic from VIM group of INRA France for generous gift of PrP^C proteins.

Reference

1. Masters CL, Gajdusek DC, Gibbs CJ (1981) Brain 104:559–588
2. Prusiner SB (1991) Science 252:1515–1522
3. Pan KM, Baldwin M, Nguen J, Gasset M, Serban A, Groth D, Mehlhorn I, Huang Z, Fletterick RJ, Cohen EF, Prusiner SB (1993) Proc Natl Acad Sci USA 90:10962–10966
4. Fournier-Wirth C, Jaffrezic-Renault N, Coste J (2010) Transfusion 50:2032–2045
5. Safar JG, Geschwind MD, Deering C, Didorenko S, Sattavat M, Sanchez H, Serban A, Vey M, Baron H, Giles K, Miller BL, Dearmond SJ, Prusiner SB (2005) Proc Natl Acad Sci USA 102:3501–3506
6. Puchtler H, Sweat F (1965) J Histochem Cytochem 13:693–694
7. Westermark GT, Johnson KH, Westermark P (1999) Meth Enzymol 309:3–25
8. Dezutter NA, Sciot RM, de Groot TJ, Bormans GM, Verbruggen AM (2001) Nuclear Med Commun 22:553–558
9. Matsuno H, Niikura K, Okahata Y (2001) Chemistry 7:3305–3312
10. Ando Y, Haraoka K, Terazaki H, Tanoue Y, Ishikawa K, Katsuragi S, Nakamura M, Sun X, Nakagawa K, Sasamoto K, Takesako K, Ishizaki T, Sasaki Y, Doh-ura K (2003) Lab Investig 83:1751–1759
11. Zerr I, Bodemer M, Gefeller O, Otto M, Poser S, Wiltfang J, Windl O, Kretzschmar HA, Weber T (1998) Ann Neurol 43:32–40
12. Kuczius T, Koch R, Keyvani K, Karch H, Grassi J, Groschup MH (2007) European J Neurosci 25:2649–2655
13. Kawatake S, Nishimura Y, Sakaguchi S, Iwaki T, Dohura K (2006) Biol Pharm Bull 29:927–932
14. Cuccioloni M, Amici M, Eleuteri AM, Biagetti M, Barocci S, Angeletti M (2005) Proteins Struct Funct Bioinform 58:728–734
15. Maissen M, Roeckl C, Glatzel M, Goldmann W, Aguzzi A (2001) Lancet 357:2026–2028
16. Hianik T, Porfirieva A, Grman I, Evtugyn G (2009) Prot Pept Lett 16:363–367
17. Scarano S, Scuffi C, Mascini M, Minunni M (2011) Anal Chim Acta 707:178–183
18. Stenberg E, Persson B, Roos H, Urbaniczky C (1991) J Coll Interf Sci 143:513–526
19. Li YJ, Bi LJ, Zhang XE, Zhou YF, Zhang JB, Chen YY, Li W, Zhang ZP (2006) Anal Bioanal Chem 386:1321–1326
20. Wan JY, Wang X, Li JP, Liu WS, Xu M, Liu LN, Xu J, Wang HY, Gao HW (2009) Arch Virol 154:1901–1908
21. Lê HQA, Sauriat-Dorizon H, Korri-Youssoufi H (2010) Anal Chim Acta 674:1–8
22. Pollet J, Delport F, Janssen KPF, Jans K, Maes G, Pfeiffer H, Wevers M, Lammertyn J (2009) Biosens Bioelectr 25:864–869
23. Ostatná V, Vaisocherová H, Homola J, Hianik T (2008) Anal Bioanal Chem 391:1861–1869
24. Lee SJ, Youn BS, Park JW, Niazi JH, Kim YS, Gu MB (2008) Anal Chem 80:2867–2873
25. Takemura K, Wang P, Vorberg I, Surewicz W, Priola SA, Kanthasamy A, Pottathil R, Chen SG, Sreevatsan S (2006) Exper Biol Med 231:204–214
26. Korri-Youssoufi H, Yassar A (2001) Biomacromolecules 2:58–64
27. Skladal P, Horacek J (1999) Anal Lett 32:1519–1529
28. Cavic BA, Thompson M (2001) Anal Chim Acta 469:101–113
29. Sauerbrey G (1959) Z Phys 155:206–210
30. Snejdárková M, Svobodova L, Polohova V, Hianik T (2008) Anal Bioanal Chem 390:1087–1091
31. Zhou XC, Huang LQ, Li SFY (2001) Biosens Bioelectr 16:85–95
32. O'Shannessy DJ, Brigham-Burke M, Soneson KK, Hensley P, Brooks I (1993) Anal Biochem 212:457–468
33. Hianik T, Grman I, Karpisova I (2009) Chem Commun 41:6303–6305
34. Neundlinger I, Poturnayova A, Karpisova I, Rankl C, Hinterdorfer P, Snejdarkova M, Hianik T, Ebner A (2011) Biophys J 101:1781–1787
35. Ryazanova AY, Kubareva EA, Grman I, Lavrova NV, Ryazanova EM, Oretskaya TS, Hianik T (2011) Analyst 136:1227–1233